

S1

Supplementary Information for

**Copper clusters built on bulky amidinate ligands:
spin delocalization via superexchange rather than direct metal–metal bonding**

Xuan Jiang, John C. Bollinger, Mu-Hyun Baik* and Dongwhan Lee*

Department of Chemistry and School of Informatics, Indiana University, Bloomington, IN 47405
Email: mbaik@indiana.edu, dongwhan@indiana.edu

Experimental Section

General Considerations. All reagents were obtained from commercial suppliers and used as received unless otherwise noted. Dichloromethane, diethyl ether, acetonitrile, and pentanes were saturated with nitrogen and purified by passage through activated Al₂O₃ columns under nitrogen (Innovative Technology SPS 400)^{S1} Hexamethyldisiloxane was distilled from CaH₂. The compounds *N,N'*-diphenylbenzamidinate (PhCN^{Ph}₂H) and *N,N'*-bis(2,6-dimethylphenyl)benzamidinate (PhCN^{Me2Ph}₂H) were synthesized according to literature procedures.^{S2} All air-sensitive manipulations were carried out under nitrogen atmosphere in a M. Braun drybox or by standard Schlenk line techniques.

[Cu₄(μ-N^{Ph}₂CPh)₄] (1). To a rapidly stirred pale yellow MeCN solution (10 mL) of PhCN^{Ph}₂H (400 mg, 1.47 mmol) at –35 °C was added dropwise n-BuLi (1.0 mL; 1.6 M in hexanes). The yellow solution was warmed up to r.t. A MeCN solution (3 mL) of [Cu(MeCN)₄](PF₆) (547 mg, 1.47 mmol) was added dropwise. The solution initially turned turbid, but quickly clarified with continued stirring. At the end of the addition, the reaction mixture remained heterogeneous. After stirring for 1 h, the solid material (427 mg, 0.32 mmol, 86%) was isolated by filtration and washed with Et₂O. Vapor diffusion of pentanes into a saturated CH₂Cl₂ solution of this material afforded yellow blocks of **1**, which were suitable for X-ray crystallography. ¹H-NMR (300 MHz, CDCl₃): δ 6.27–7.10 (m, 60H); ¹³C-NMR (75 MHz, CDCl₃): δ 121.74, 122.54, 126.05, 126.47, 127.62, 128.06, 128.36, 128.61, 131.50, 134.90, 149.79, 169.21. FT-IR (KBr, cm⁻¹) 3058, 3029, 1593, 1579, 1478, 1440, 1265, 1206, 1170, 1132, 1074, 1026, 998, 942, 924, 890, 789, 779, 762, 742, 710, 691, 517. Anal. Calcd for C₇₆H₆₀Cu₄N₈: C, 68.14; H, 4.51; N, 8.37. Found: C, 68.16; H, 5.11; N, 8.29.

[Cu₂(μ-N^{Me2Ph}₂CPh)₂] (2). This compound was prepared from [Cu(MeCN)₄](PF₆) (559 mg, 1.50 mmol) and PhCN^{Me2Ph}₂H (493 mg, 1.50 mmol) by a procedure analogous to that used to prepare **1** (538 mg, 0.69 mmol, 91%). Pale yellow blocks of **2** were obtained by recrystallization from CH₂Cl₂/pentanes at r.t. and analyzed by X-ray crystallography. ¹H-NMR (300 MHz, CDCl₃): δ 2.35 (s, 24H), 6.62–6.90 (m, 22H); ¹³C-NMR (75 MHz, CDCl₃): δ 19.96, 123.83, 126.52, 127.51, 128.18, 128.31, 133.01, 135.46, 146.68. FT-IR (KBr, cm⁻¹) 3057, 3038, 2915, 2849, 1491, 1436, 1375, 1265, 1193, 1092, 1028, 981, 958, 941, 808, 781, 758, 700, 515. Anal. Calcd for C₄₆H₄₆Cu₂N₄: C, 70.65; H, 5.93; N, 7.16. Found: C, 70.59; H, 5.89; N, 7.00.

[Cu₂(μ-N^{Me2Ph}₂CPh)₂(MeCN)₂](SbF₆) (3a). A pale yellow CH₂Cl₂ solution (3 mL) of **2** (101 mg, 0.129 mmol) was treated with MeCN (100 μL) and a CH₂Cl₂ (1 mL) suspension of AgSbF₆ (45 mg, 0.131 mmol) was added with rapid stirring. The color of the reaction mixture turned dark bluish green following the addition. The solution was stirred for 5 min and filtered through Celite. Dark purple microcrystals of **3a** (104 mg, 0.0946 mmol, 73%) were obtained by layering pentanes over the filtrate at –35 °C. Recrystallization from 1,2-dichloroethane/pentanes at –35 °C afforded thin plates, which were suitable for X-ray crystallography. FT-IR (KBr, cm⁻¹) 3063, 3019, 2927, 2303, 2275, 2254, 1605, 1568, 1488, 1440, 1377, 1261, 1237, 1185, 1092, 1029, 946, 812, 785, 772, 761, 732, 707, 658, 513. Anal. Calcd for C₅₀H₅₂Cu₂F₆N₆Sb: C, 54.60; H, 4.77; N, 7.64. Found: C, 54.32; H, 4.97; N, 7.04.

[Cu₂(μ-N^{Me2Ph}₂CPh)₂(THF)₂](SbF₆) (3b). This compound was prepared in a manner similar to that described for **3a**, except that THF was added instead of MeCN. Dark violet crystals of **3b** (49%) were obtained by layering pentanes over the reaction mixture at –35 °C, which were suitable for X-ray crystallography. FT-IR (KBr, cm⁻¹) 3315, 3058, 3015, 2922, 2856, 1604, 1585, 1565, 1483, 1437, 1378, 1260, 1230, 1187, 1097, 1023, 941, 859, 774,

704, 659, 524. Anal. Calcd for C₅₄H₆₂Cu₂F₆N₄O₂Sb: C, 55.82; H, 5.38; N, 4.82. Found: C, 55.97; H, 5.26; N, 5.37.

Physical Measurements. ¹H-NMR and ¹³C-NMR spectra were recorded on a Varian Gemini 2000 NMR spectrometer (300 MHz). Chemical shifts were reported versus tetramethylsilane and referenced to the residual solvent peaks. FT-IR spectra were recorded on a Nicolet 510P FT-IR spectrometer with EZ OMNIC E.S.P. software. Solid samples were pressed into KBr pellets. UV-vis spectra were recorded on a Perkin-Elmer Lambda 19 UV/vis/near-IR spectrometer. Electrochemical studies were carried out under nitrogen with an Autolab model PGSTAT30 potentiostat (Eco Chemie). A three-electrode configuration consisting of a platinum button as the working electrode, a Ag/AgNO₃ (0.01 M in MeCN with 0.1 M (n-Bu₄N)PF₆) reference electrode, and a platinum coil counter electrode was used. The supporting electrolyte was either 0.2 M (n-Bu₄N)ClO₄ or (n-Bu₄N)PF₆ in CH₂Cl₂. All electrochemical potentials are reported to the Cp₂Fe/Cp₂Fe⁺ redox couple.

EPR Spectroscopy. X-band EPR spectra were recorded on a Bruker EMX-A spectrometer with an ER041X microwave bridge. Liquid helium temperatures were maintained with an Oxford ESR900 continuous flow cryostat and liquid nitrogen temperature with an EPR finger dewar. For all measurements, 5 mM frozen solution samples were prepared in CH₂Cl₂/toluene (1:1, v/v). Simulations were carried out with the W95EPR program. The fits incorporated coupling of the unpaired spin simultaneously to each $I = 3/2$ copper center.

DFT Calculations

All calculations were carried out using Density Functional Theory as implemented in the Jaguar 5.5 suite^{S3} of ab initio quantum chemistry programs. Geometry optimizations were performed with the B3LYP^{S4-7} functional and the 6-31G** basis set. Cu was represented using the Los Alamos LACVP** basis.^{S8-10} The energies of the optimized structures were reevaluated by additional single-point calculations on each optimized geometry using Dunning's correlation-consistent triple- ξ basis set^{S11} cc-pVTZ(-f) that includes a double set of polarization functions. For Cu, we used a modified version of LACVP**, designated as LACV3P**, in which the exponents were decontracted to match the effective core potential with the triple- ξ . Vibrational frequency calculations based on analytical second derivatives at the B3LYP/6-31G** (LACVP**) level of theory were carried out on smaller models, to derive the zero-point-energy (ZPE) and entropy corrections at room temperature utilizing unscaled frequencies. Note that by entropy here we refer specifically to the vibrational/rotational/translational entropy of the solute(s); the entropy of the solvent is implicitly included in the dielectric continuum model. The molecules used for vibrational frequency calculations are derived from the corresponding fully optimized structure by replacing the aromatic substituents of the amidinate ligand with methyl groups. Evaluating the frequencies on the original model is impossible due to enormous technical demands. Using smaller core models to obtain differential entropies for redox reactions of this type is a reasonable approach. These methyl models are denoted **2-Me** below.

Solvation energies were evaluated by a self-consistent reaction field (SCRF)^{S12-14} approach based on accurate numerical solutions of the Poisson-Boltzmann equation.^{S15} In the results reported, solvation calculations were carried out at the optimized gas-phase geometry employing the dielectric constant of $\epsilon = 9.08$ (methylene chloride) to match the experimental conditions. As is the case for all continuum models, the solvation energies are subject to empirical parameterization of the atomic radii that are used to generate the solute surface. We employ the standard set^{S15} of optimized radii in Jaguar for H (1.150 Å), C (1.900 Å), N (1.600 Å), O (1.600 Å). We make use of the metallic van der Waals radii 1.748 Å for Cu.

The energy component have been computed following the protocol of our previous work (ref. S16). The electron attachment free energy in solution phase $\Delta G^{\text{EA}}(\text{sol})$ and the redox potentials($E_{1/2}$) for the reactions were calculated as follows:^{S16}

$$\Delta G^{\text{EA}}(\text{sol}) = \Delta G^{\text{EA}}(\text{gas}) + \Delta G^{\text{solv}} \quad (1)$$

$$\Delta G^{\text{EA}}(\text{gas}) = \Delta H^{\text{EA}}(\text{gas}) - T\Delta S(\text{gas}) \quad (2)$$

$$\Delta H^{\text{EA}}(\text{gas}) = \Delta H^{\text{EA}}(\text{SCF}) + \Delta ZPE + \Delta U \quad (3)$$

$$\Delta G^{\text{EA}}(\text{sol}) = -nFE_{1/2} \quad (4)$$

$\Delta G^{\text{EA}}(\text{gas})$ = electron attachment free energy in gas phase; ΔG^{solv} = free energy of solvation as computed using the continuum solvation model; $\Delta H^{\text{EA}}(\text{gas})$ = electron attachment enthalpy in gas phase; T = temperature (298.15K);

$\Delta S(\text{gas})$ = entropy difference in gas phase; $\Delta H^{\text{EA}}(\text{SCF})$ = self consistent field energy, i.e. “raw” electronic energy as computed from the SCF procedure; ΔZPE = zero point energy difference; ΔU = internal energy correction; F = Faraday constant; n = number of electrons.

For the standard hydrogen electrode (SHE), the absolute potential has been determined experimentally to be 4.43 eV,^{S17} thus to compare the computed absolute potentials with the experimental potentials referenced to the SHE, 4.43 eV has to be subtracted. Experimental potentials in this study have been measured against the Fc/Fc^+ couple (+0.5512 V vs. SHE), thus to obtain the potentials relative to Fc/Fc^+ , we subtract 4.9812 V from the absolute potentials that we computed using DFT.

References

- (S1) Pangborn, A. B.; Giardello, M. A.; Grubbs, R. H.; Rosen, R. K.; Timmers, F. J. *Organometallics* **1996**, *15*, 1518.
(S2) Ogata, S.-i.; Mochizuki, A.; Kakimoto, M.-a.; Imai, Y. *Bull. Chem. Soc. Jpn.* **1986**, *59*, 2171.
(S3) Jaguar. 5.5 ed, Schrödinger, L.L.C, Portland, OR, 1991-2003.
(S4) Becke, A. D. *Phys. Rev. A* **1988**, *38*, 3098.
(S5) Becke, A. D. *J. Chem. Phys.* **1993**, *98*, 5648.
(S6) Lee, C. T.; Yang, W. T.; Parr, R. G. *1988 Phys. Rev. B*, *37*, 785.
(S7) Vosko, S. H.; Wilk, L.; Nusair, M. *Can. J. Phys.* **1980**, *58*, 1200.
(S8) Hay, P. J.; Wadt, W. R. *J. Chem. Phys.* **1985**, *82*, 270.
(S9) Hay, P. J.; Wadt, W. R. *J. Chem. Phys.* **1985**, *82*, 299.
(S10) Wadt, W. R.; Hay, P. J. *J. Chem. Phys.* **1985**, *82*, 284.
(S11) Dunning, T. H. *J. Chem. Phys.* **1989**, *90*, 1007.
(S12) Marten, B.; Kim, K.; Cortis, C.; Friesner, R. A.; Murphy, R. B.; Ringnalda, M. N.; Sitkoff, D.; Honig, B. *J. Phys. Chem.* **1996**, *100*, 11775.
(S13) Friedrichs, M.; Zhou, R. H.; Edinger, S. R.; Friesner, R. A. *J. Phys. Chem. B* **1999**, *103*, 1190.
(S14) Edinger, S. R.; Cortis, C.; Shenkin, P. S.; Friesner, R. A. *J. Phys. Chem. B* **1997**, *101*, 1190.
(S15) Rashin, A. A.; Honig, B. *J. Phys. Chem.* **1985**, *89*, 5588.
(S16) Baik, M. H.; Friesner, R. A. *J. Phys. Chem. A* **2002**, *106*, 7407.
(S17) Reiss, H.; Heller, A. *J. Phys. Chem.* **1985**, *89*, 4207.

List of Tables

- Table S1** DFT optimized structures.
Table S2 Computed energy components and potentials vs Fc/Fc^+ couple.
Table S3 Atomic Spin Densities from Mulliken analysis for 2^+ .

List of Figures

- Fig. S1** Cyclic voltammograms (scan rate = 50 mV/sec) and square wave voltammograms (step potential = 5 mV; square wave frequency = 10 Hz; square wave amplitude = 20 mV) of $[\text{Cu}_2(\mu\text{-N}^{\text{Me}_2\text{Ph}}_2\text{CPh})_2]$ (**2**) in CH_2Cl_2 with 0.2 M $(\text{Bu}_4\text{N})(\text{ClO}_4)$ as supporting electrolyte.
Fig. S2 ORTEP diagrams of the cation in $[\text{Cu}_2(\mu\text{-N}^{\text{Me}_2\text{Ph}}_2\text{CPh})_2(\text{THF})_2](\text{SbF}_6)$ (**3b**) with thermal ellipsoids at 50% probability: top, molecule 1; bottom, molecule 2.
Fig. S3 X-band EPR spectra of a frozen CH_2Cl_2 /toluene (1:1, v/v) solution sample of $[\text{Cu}_2(\mu\text{-N}^{\text{Me}_2\text{Ph}}_2\text{CPh})_2(\text{MeCN})_2](\text{SbF}_6)$ (**3a**) measured at 40 K (·····), 20 K (-----), and 4.5 K (—), respectively.

- Fig. S4** ORTEP diagram of $[\text{Cu}_4(\mu\text{-N}^{\text{Ph}}_2\text{CPh})_4]$ (**1**) with thermal ellipsoids at 50% probability: top, whole molecule; bottom, core structure.
- Fig. S5** ORTEP diagram of $[\text{Cu}_2(\mu\text{-N}^{\text{Me}2\text{Ph}}_2\text{CPh})_2]$ (**2**) with thermal ellipsoids at 50% probability.
- Fig. S6** ORTEP diagram of the cation in $[\text{Cu}_2(\mu\text{-N}^{\text{Me}2\text{Ph}}_2\text{CPh})_2(\text{MeCN})_2](\text{SbF}_6)$ (**3a**) with thermal ellipsoids at 50% probability.

Supplementary Material (ESI) for Chemical Communications
 # This journal is © The Royal Society of Chemistry 2005

Table S1. DFT Optimized Structures.

=====			H	-3.623091522	-4.004962547	-3.528655076	
2			C	-2.980239795	-2.953784094	-1.127038534	
=====			C	0.138349946	-4.080891797	-0.063836529	
Cu	-0.092088996	-0.007946420	1.162063753	C	-0.561479041	-4.845896060	0.880372450
Cu	-0.084040875	0.006877611	-1.277767415	H	-1.183685217	-4.351527114	1.617132544
N	-0.356257496	1.903426774	1.077493372	C	-0.471401528	-6.236612136	0.877202403
C	-0.932255555	2.509768067	2.235693526	H	-1.025802077	-6.812541973	1.612909274
C	-2.281349745	2.931396968	2.235115908	C	0.330942944	-6.885162708	-0.061512939
C	-2.822954709	3.457674118	3.413353610	H	0.405937030	-7.969158115	-0.060076074
C	-2.066660414	3.551103681	4.578465077	C	1.036952224	-6.134483851	-1.001859000
C	-0.751012927	3.092992953	4.581252272	H	1.665763025	-6.630307231	-1.736154587
C	-0.170215484	2.559482141	3.427453757	C	0.936330470	-4.744287969	-1.007270770
C	-0.104985688	2.581493075	-0.051186660	H	1.487080232	-4.170637395	-1.743633141
N	0.138702056	1.917208511	-1.188611490	C	-0.094143678	4.086270022	-0.045137200
C	0.729483789	2.523583940	-2.339106261	C	0.657024878	4.794258368	0.904573395
C	-0.024565710	2.583435041	-3.535242658	H	1.233838600	4.253029697	1.645457620
C	0.568594621	3.112475917	-4.685001491	C	0.677764489	6.187802058	0.899449403
C	1.888935138	3.555963928	-4.673891163	H	1.271319548	6.718804644	1.638549111
C	2.637310806	3.451220386	-3.505211589	C	-0.062487846	6.897052832	-0.046702739
C	2.083944445	2.928718138	-2.330924888	H	-0.049223064	7.983587147	-0.047944888
C	-3.149030528	2.786704067	1.007108792	C	-0.819437998	6.203964889	-0.991822460
H	-3.859874123	3.786523224	3.412865406	H	-1.400111865	6.747412039	-1.732274985
H	-2.504300791	3.964096106	5.483423725	C	-0.830004597	4.810111662	-0.995200732
H	-0.159814750	3.145685613	5.492904933	H	-1.417555188	4.280846971	-1.736708950
C	1.244604923	2.030920020	3.472808826	H	-4.207146405	2.871144991	1.271983048
C	-1.442784143	2.065357090	-3.587283978	H	-2.933970875	3.558345559	0.258477985
H	-0.016246239	3.171866154	-5.599896556	H	-2.990394783	1.816834098	0.523530416
H	2.336574635	3.964953675	-5.575489378	H	1.706162300	2.241625917	4.442227919
H	3.677971234	3.767030483	-3.499083619	H	1.273235270	0.942958379	3.321650905
C	2.945802357	2.768408506	-1.101093306	H	1.880027772	2.462362900	2.691141158
N	0.238912317	-1.901779268	1.079967871	H	-1.890008817	2.257432709	-4.566966554
C	0.853183296	-2.471117220	2.236686770	H	-1.480720836	0.981360194	-3.409872586
C	2.229105758	-2.795788012	2.241873659	H	-2.084738779	2.519162154	-2.823886982
C	2.801982466	-3.279731354	3.423248819	H	4.005461959	2.839058493	-1.363056202
C	2.050061999	-3.423816467	4.585701201	H	2.739223796	3.540634382	-0.351239164
C	0.705258772	-3.059706991	4.582869899	H	2.773221822	1.799091370	-0.620752684
C	0.092600878	-2.571566213	3.425759373	H	4.150535625	-2.597974762	1.289902476
C	0.041243384	-2.579267062	-0.058381435	H	2.936000660	-3.374252742	0.269574271
N	-0.241054976	-1.917200531	-1.189283700	H	2.866143150	-1.633165261	0.534346951
C	-0.777423833	-2.558602882	-2.347601914	H	-1.800001162	-2.355726300	4.437682799
C	-0.008891572	-2.571055845	-3.536033275	H	-1.454274914	-1.058279732	3.284657111
C	-0.554082285	-3.143000741	-4.689061714	H	-1.959841806	-2.628308169	2.692765277
C	-1.841727842	-3.675024864	-4.688437266	H	1.849826546	-2.150836938	-4.545961007
C	-2.606563499	-3.618133811	-3.526944499	H	1.341613733	-0.875219829	-3.431284001
C	-2.100423450	-3.055872207	-2.350266122	H	2.030236663	-2.356134298	-2.794144933
C	3.090817510	-2.589440728	1.018931755	H	-4.030243124	-3.101057894	-1.395453052
H	3.859739562	-3.533225656	3.427793833	H	-2.724632998	-3.706529148	-0.372332285
H	2.512803351	-3.801610006	5.493272901	H	-2.880018351	-1.973236444	-0.649696140
H	0.116543397	-3.150053925	5.492913910	=====			
C	-1.354231745	-2.137859499	3.462722326	2(+)	=====		
C	1.374269480	-1.963582763	-3.578766484	Cu	-0.003577995	-0.004152362	1.078937603
H	0.043074262	-3.167348934	-5.597961967	Cu	0.015046201	-0.005509802	-1.279911180
H	-2.251367095	-4.117114152	-5.592491183	N	-0.093176377	1.883212697	1.077324882
=====			C	-0.526554488	2.386712624	2.333378883	

Supplementary Material (ESI) for Chemical Communications
This journal is © The Royal Society of Chemistry 2005

H	0.576530095	-4.488033837	-0.999106472	C	0.263740865	-4.073229495	-0.076753927
H	-0.711470780	-4.517930596	0.209763489	C	-0.295968402	4.075813037	-0.063691604
H	0.972475272	-4.415464404	0.718300854	H	0.617972585	3.388788115	2.401268117
H	-0.732189352	4.461316475	-0.976870922	H	0.042616249	1.903855921	3.192375581
H	0.651660745	4.546410739	0.116464703	H	-1.123445587	3.066631826	2.531994135
H	-0.981546831	4.409229383	0.766952664	H	0.590302249	3.414345491	-2.490555528
<hr/>							
2-Me(+)							
<hr/>							
Cu	0.021727387	0.003574415	1.196941212	H	0.062091764	-1.878126908	3.202301142
Cu	-0.012348432	0.001108126	-1.308667270	H	1.115930963	-3.122723338	2.500986447
N	-0.123304749	1.885091428	1.103745558	H	-0.654559598	-3.363118353	-2.507071073
C	-0.163232252	2.625507528	2.370303691	H	1.100458839	-3.132219053	-2.588947794
C	-0.188408754	2.561601333	-0.053342979	H	0.016670238	-1.918980245	-3.300972890
N	-0.111001095	1.885390286	-1.210681718	H	1.029893897	-4.400380777	-0.784590807
C	-0.129594842	2.627589706	-2.476378684	H	-0.690869044	-4.498191893	-0.411080769
N	0.123263381	-1.880753103	1.106262980	H	0.498673658	-4.503157827	0.893371889
C	0.154260382	-2.615660968	2.376343668	H	-0.896349309	4.427698394	-0.903563817
C	0.169299899	-2.559216750	-0.050803673	H	0.703671237	4.520370434	-0.160328954
N	0.102629476	-1.882365844	-1.207853934	H	-0.743584591	4.461494138	0.850989364
C	0.101252465	-2.632463016	-2.468356395				
C	0.272884591	-4.066759233	-0.071631330				
C	-0.316423517	4.067945186	-0.055649739				
H	0.602783954	3.408003893	2.413317442				
H	0.019179372	1.933042415	3.193192474				
H	-1.143648657	3.090266002	2.536875922				
H	0.609951214	3.435431069	-2.493815665				
H	-1.118698184	3.060704657	-2.675342327				
H	0.102293305	1.942876265	-3.293449462				
H	-0.641537374	-3.367218568	2.433959847				
H	0.008323010	-1.911886142	3.197205153				
H	1.118004423	-3.114840161	2.534274240				
H	-0.702577878	-3.377901307	-2.498849804				
H	1.054545870	-3.150002472	-2.635685560				
H	-0.050790480	-1.940406310	-3.297458816				
H	0.958855811	-4.398552645	-0.853527212				
H	-0.707504774	-4.508962630	-0.286154321				
H	0.622510387	-4.474056047	0.874805436				
H	-0.868619764	4.424250557	-0.924873896				
H	0.679218327	4.528541451	-0.083295271				
H	-0.824236092	4.432354428	0.836320319				
<hr/>							
2-Me(2+)							
<hr/>							
Cu	0.011197167	0.003401063	1.209602769				
Cu	-0.018190812	0.000572435	-1.320498257				
N	-0.117291481	1.876203311	1.097629641				
C	-0.141621738	2.598213579	2.372860656				
C	-0.187386232	2.575945519	-0.053563183				
N	-0.125424619	1.874752465	-1.205985961				
C	-0.147979371	2.604177828	-2.476174199				
N	0.124316021	-1.871167216	1.102801234				
C	0.164593900	-2.587508231	2.381342242				
C	0.171108034	-2.572932093	-0.048264387				
N	0.108815690	-1.872132108	-1.202081428				
C	0.142046724	-2.608682419	-2.466967057				

Table S2. Computed energy components and potentials vs Fc/Fc⁺ couple.

* denotes values derived from the small models **2-Me(n+)**; n = 0, 1, 2

	2	2(+)	2(2+)
E(SCF) [eV]	-65102.454	-65096.029	-65086.997
G(Solv) [kcal/mol]	-10.03	-33.19	-102.67
U* [kcal/mol]	11.53	11.34	11.80
ZPE* [kcal/mol]	166.73	167.19	166.45
S* [e.u.]	139.96	139.24	142.30
-(298.15K)S* [kcal/mol]	-41.73	-41.51	-42.43
G(Sol) [eV]	-65096.969	-65091.527	-65085.559

	$\Delta G(\text{Sol})$ [eV]	E1/2 (Calc) [V]	E1/2 (Exp) [V]
2 => 2(+)	5.442	0.461	0.31
2(+) => 2(2+)	5.967	0.986	0.79
Difference		0.525	0.48

Supplementary Material (ESI) for Chemical Communications
This journal is © The Royal Society of Chemistry 2005

Table S3. Atomic Spin Densities from Mulliken analysis for 2⁺. See Table S1 for the Coordinates of 2⁺.

Atom	Cu1	Cu2	N3	C4	C5
Spin	0.22348	0.20390	0.06408	0.02016	0.03603
Atom	C6	C7	C8	C9	C10
Spin	-0.01926	0.06207	-0.01823	0.03383	-0.00028
Atom	N11	C12	C13	C14	C15
Spin	0.04841	0.01189	0.01483	-0.00805	0.02979
Atom	C16	C17	C18	H19	H20
Spin	-0.00911	0.01852	-0.00282	0.00066	-0.00289
Atom	H21	C22	C23	H24	H25
Spin	0.00070	-0.00326	-0.00086	0.00027	-0.00138
Atom	H26	C27	N28	C29	C30
Spin	0.00050	-0.00150	0.06601	0.01990	0.03690
Atom	C31	C32	C33	C34	C35
Spin	-0.01979	0.06371	-0.01896	0.03506	-0.00029
Atom	N36	C37	C38	C39	C40
Spin	0.05048	0.01262	0.01585	-0.00875	0.03179
Atom	C41	C42	C43	H44	H45
Spin	-0.00970	0.01938	-0.00297	0.00069	-0.00297
Atom	H46	C47	C48	H49	H50
Spin	0.00073	-0.00337	-0.00094	0.00029	-0.00148
Atom	H51	C52	C53	C54	H55
Spin	0.00053	-0.00158	0.00052	-0.00038	-0.00002
Atom	C56	H57	C58	H59	C60
Spin	0.00027	0.00003	-0.00079	0.00004	0.00021
Atom	H61	C62	H63	C64	C65
Spin	0.00005	0.00000	0.00003	0.00043	-0.00036
Atom	H66	C67	H68	C69	H70
Spin	-0.00001	0.00027	0.00002	-0.00073	0.00003
Atom	C71	H72	C73	H74	H75
Spin	0.00019	0.00005	0.00007	0.00003	0.00049
Atom	H76	H77	H78	H79	H80
Spin	0.00201	0.00100	0.00000	0.00051	0.00141
Atom	H81	H82	H83	H84	H85
Spin	0.00014	-0.00035	0.00065	0.00017	0.00101
Atom	H86	H87	H88	H89	H90
Spin	0.00045	0.00047	0.00207	0.00113	0.00001
Atom	H91	H92	H93	H94	H95
Spin	0.00056	0.00145	0.00014	-0.00032	0.00069
Atom	H96	H97	H98		
Spin	0.00019	0.00104	0.00046		

Fig. S1 Cyclic voltammograms (scan rate = 50 mV/sec) and square wave voltammograms (step potential = 5 mV; square wave frequency = 10 Hz; square wave amplitude = 20 mV) of $[\text{Cu}_2(\mu\text{-N}^{\text{Me}_2\text{Ph}}_2\text{CPh})_2]$ (**2**) in CH_2Cl_2 with 0.2 M $(\text{Bu}_4\text{N})(\text{ClO}_4)$ as supporting electrolyte.

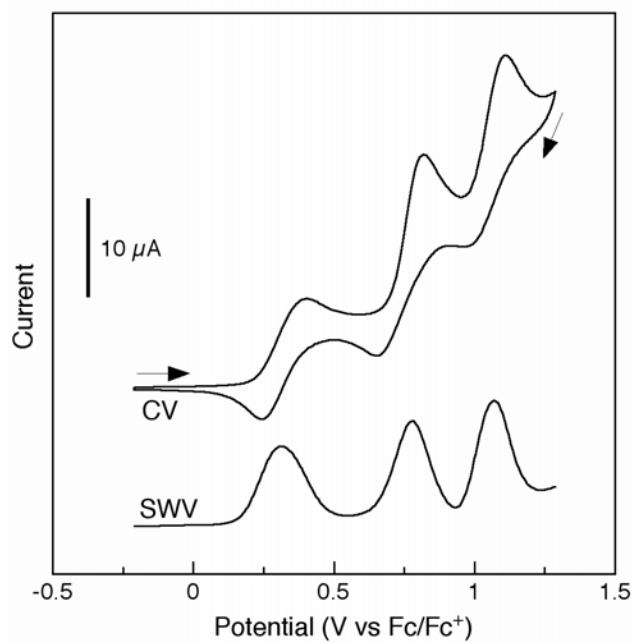


Fig. S2 ORTEP diagrams of the cation in $[\text{Cu}_2(\mu\text{-N}^{\text{Me}_2\text{Ph}}_2\text{CPh})_2(\text{THF})_2](\text{SbF}_6)$ (**3b**) with thermal ellipsoids at 50% probability: left, molecule 1; right, molecule 2.

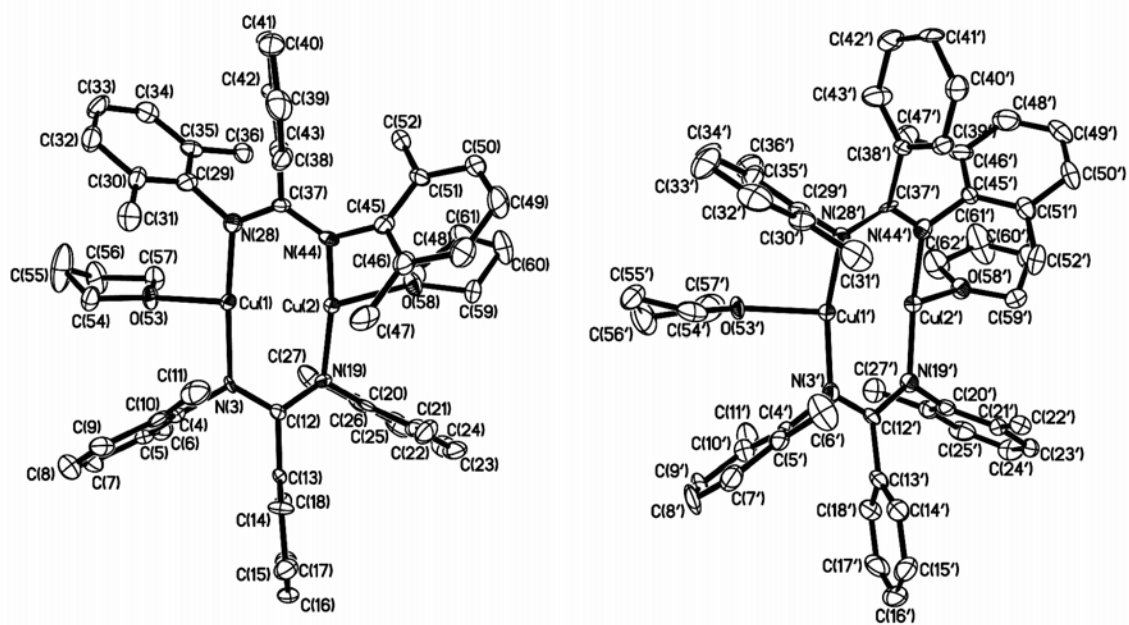


Fig. S3 X-band EPR spectra of a frozen CH_2Cl_2 /toluene (1:1, v/v) solution sample of $[\text{Cu}_2(\mu\text{-N}^{\text{Me}2\text{Ph}}_2\text{CPh})_2(\text{MeCN})_2](\text{SbF}_6)$ (**3a**) measured at 40 K (·····), 20 K (-----), and 4.5 K (—), respectively.

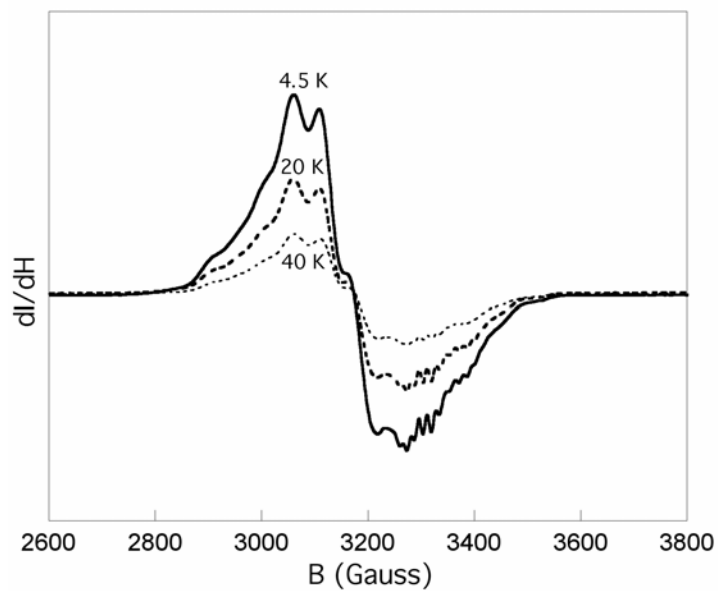


Fig. S4 ORTEP diagram of $[\text{Cu}_4(\mu\text{-N}^{\text{Ph}}_2\text{CPh})_4]$ (**1**) with thermal ellipsoids at 50% probability: left, whole molecule; right, core structure.

Supplementary Material (ESI) for Chemical Communications
This journal is © The Royal Society of Chemistry 2005

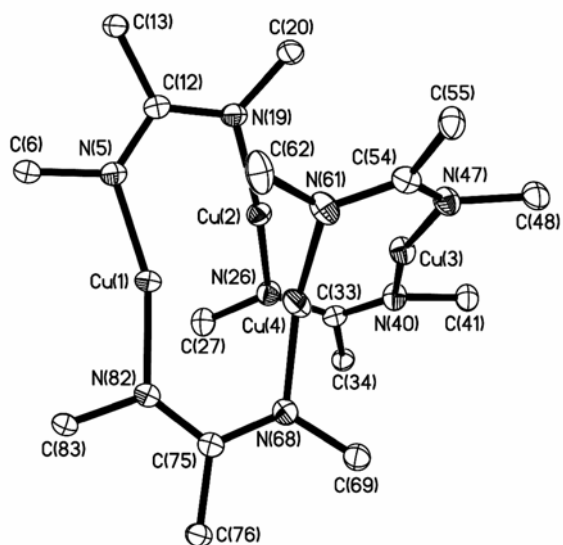
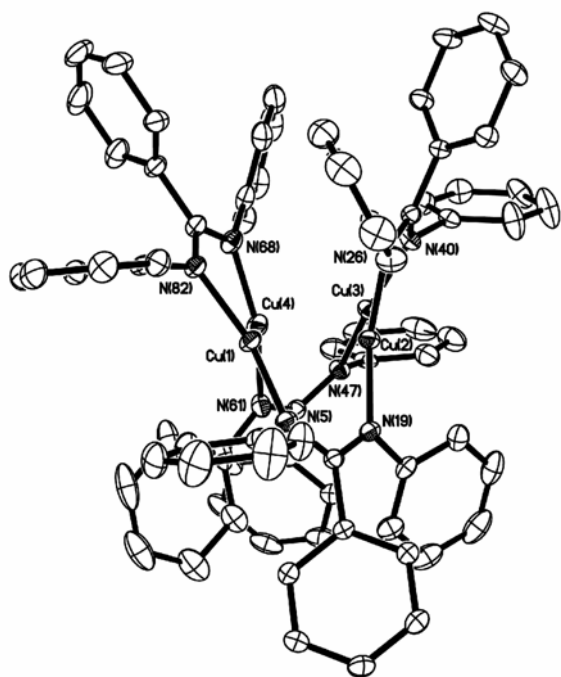


Fig. S5 ORTEP diagram of $[\text{Cu}_2(\mu\text{-N}^{\text{Me2Ph}}_2\text{CPh})_2]$ (**2**) with thermal ellipsoids at 50% probability.

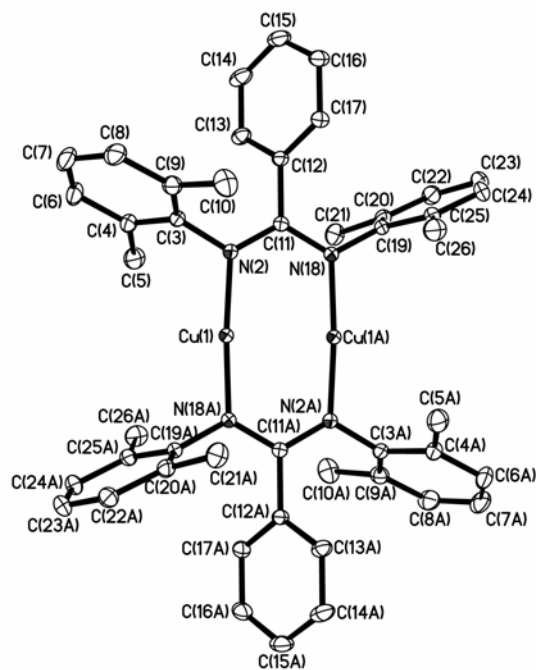


Fig. S6 ORTEP diagram of the cation in $[\text{Cu}_2(\mu\text{-N}^{\text{Me2Ph}}_2\text{CPh})_2(\text{MeCN})_2](\text{SbF}_6)$ (**3a**) with thermal ellipsoids at 50% probability.

Supplementary Material (ESI) for Chemical Communications
This journal is © The Royal Society of Chemistry 2005

